To cite this version :

Thermal Aging Effects on Overall Mechanical Behavior of Short Glass Fiber-Reinforced Polyphenylene Sulfide Composites

Peiyuan Zuo [ID]**,**[1] **Joseph Fitoussi,**[1] **Mohammadali Shirinbayan,**[1] **Farid Bakir,**[2] **Abbas Tcharkhtchi**[1]

[1]*Arts et Métiers ParisTech, PIMM – UMR CNRS 8006, 151 Boulevard de l'Hôpital, 75013, Paris, France*
[2]*Arts et Métiers ParisTech, Dynfluid, 151 Boulevard de l'Hôpital, 75013, Paris, France*

In this article, the overall mechanical properties of a short glass fiber-reinforced polyphenylene sulfide (PPS) composite were tested after oxidation at different temperatures (140, 160, 180, and 200°C), with a maximum oxidation time of approximately 5,300 h. In aspect of thermal aging process, the oxidation rates in 200 and 180°C are considerably harsher and faster than the case in 160 and 140°C, according to the concentration evolution of [C=O]. In aspect of mechanical properties, for virgin samples, due to an excellent fiber–matrix adhesion, no progressive damage is developed. Moreover, the fatigue results of aged samples show that the fatigue lifetime of PPS composites decreases more and more obviously with the oxidation time increasing while no significant loss of stiffness is observed. In addition, both monotonic and cyclic loadings are basically driven by the PPS matrix deformation. In the end, the relationship between fatigue lifetime and concentration of [CO] is built and discussed. POLYM. ENG. SCI., 59:765–772, 2019. © 2018 Society of Plastics Engineers

INTRODUCTION

In the past several decades, glass fiber-reinforced polyphenylene sulfide (PPS) composites are widely used to lighten automotive parts and other application sections [1–15]. The main reason to use this thermoplastic composite is that the sulfur atom is attached to the contraposition of benzene ring, which makes it rigid and displays some special features. For example, PPS has a short-term heat distortion temperature of 260°C. Furthermore, PPS has high stiffness and strength, as well as good stability against water, acid and many other chemicals [1–4,16–18]. The composite under study is a short glass fiber composite with a PPS matrix which is a high performance thermoplastic. One of the applications of PPS composite is to use as an inlet tank which is exposed to hot air. In this case both of thermal and mechanical properties are very important. Due to PPS matrix properties, this composite has many advantages to other equivalent composites such as high thermal stability, excellent humidity-proof ability and good mechanical properties.

In aspect of thermal oxidation of PPS, there are a wide range of reports published in the past several decades. Ehlers et al. [6] clarified in depth about the crosslinking and oxidation process of PPS. They gave extensive research about cleavage of carbon–sulfur bonds and abstraction of hydrogen process from the other rings. Similarly, some research concluded also the thermal oxidation mechanism of PPS involving a combination of crosslinking, chain scission and oxidation reactions [19]. During the same earlier period, Christopher et al. [5] studied thermal degradation of PPS by a weight loss method. They indicated that in a closed system, PPS broke down by chain-scission and transferred reactions. In another research domain, it was reported that thermal treating or annealing can affect the mechanical properties of PPS. For example, Scobbo and Hwang [20] studied the annealing effects on PPS by dynamic mechanical analysis. Annealing was performed in a vacuum oven at temperatures of 160–220°C. Annealing time was constant at 4 h. They found an increased modulus accompanied by an increase in the glass transition temperature. Other reports studied the effect of thermal treatment on the tensile and in-plane shear behavior of carbon fiber-reinforced PPS composite specimens. They found the mechanical properties have shown an appreciable degradation and the observed degradation enhanced with increasing treatment temperature and time [21]. Also some investigations utilized different methodologies to study thermal degradation of PPS. For example, Perng [22] studied thermal decomposition of PPS by stepwise (pyrolysis/gas chromatography/mass spectrometry) and (thermogravity/mass spectroscopy) methods; they clarified the mechanism and kinetic model for thermal decomposition of PPS. Cao and Chen [23] used calorimetry to record the coefficient of thermal expansion and tensile modulus of PPS composites under thermal cycling. They indicated that thermal cycling at high temperatures can increase the degree of crystallinity of PPS. These literatures give us a good reference about the degradation of PPS polymer and its reinforced parts.

As a good engineering thermoplastic material, PPS/GF composites show excellent mechanical properties and fatigue performance. In fact, there are a wide range of reports concerning this issue [24–33]. Some researchers pay attention to PPS composites with different types of reinforcements. For example, some authors studied the fatigue behavior of a carbon fabric-reinforced PPS. They concluded that PPS composite with the fiber orientations of 0 and 90° did not show significant stiffness reduction and the materials showed a very brittle failure [27]. These authors moved further to examine the inter-laminar behavior of a carbon fabric reinforced PPS by using lap experiments and they considered several loading conditions. The results showed that no crack growth was observed [25,26], both under quasi-static loading until failure and successive loading-unloading stages with increasing maximum load. Kytýr et al. [34] also evaluated impact damage effect on residual fatigue life of PPS composites reinforced by carbon fibers. They revealed that elasticity modulus decreased according to the result of three-point bending test. Moreover, frequencies, ultrasound wave propagation and bending stiffness were shown to be suitable indicators to evaluate material degradation process in carbon fiber-reinforced PPS composite during fatigue. In addition, S-N curves were studied in PPS composite systems to explore the fatigue behavior and lifetime. For example, Zhou et al. [24]

investigated the fatigue behavior of PPS- polyphenylene ether ketone blends. They found the S-N curves shifted their trends obviously for maximum cyclic stress. Mandell et al. [30] compared fatigue behavior of glass and carbon fiber reinforced PPS and both S-N curves appeared linear trends.

To assess the reliability of composite structures, Weibull distribution function has been widely used by different researchers [35–37]. For example, the statistical analysis of fatigue life using two-parameter Weibull distribution function was carried out by Bedi and Chandra [38] and they characterized fatigue life by probability density and cumulative distribution functions. Similarly, S-N curves at specific reliability levels were studied by statistical analysis in the reference of [39]. The authors showed that the stiffness-based degradation and S-N curves were correlated and can be studied by statistical analysis.

Literature review provides a lot of information about general properties of PPS and PPS/GF composites. However, PPS/GF fatigue response under thermal aging condition is lacking. Indeed, in practice, PPS/GF composites materials are used for long time service under a harsh temperature or environment. As a result, it is meaningful to propose some innovative works to get a better understanding of thermal aging effects on microstructure and mechanical properties, especially on fatigue behavior. This kind of investigation is very important to industrial applications. Therefore, this study pays attention to analyze the mechanical properties of PPS/GF composites after thermal aging.

More specifically, the first part of the present paper concerns thermal aging effect analysis. After that, quasi-static loading responses of virgin and aged samples are analyzed. In the next part, tensile tests until failure and loading-unloading with progressive increase of the maximum stress are performed on a PPS/GF composite. Thermal aging effect on fatigue properties of PPS/GF is also followed. Finally, an important issue of this work is to propose a clear relationship between thermal oxidation (e.g., [C=O]) and the principal mechanical properties (e.g., tensile strength, relative Young's modulus, fatigue lifetime) of PPS/GF composites.

MATERIAL AND METHODS

Sample Preparation

The material used for this study is a PPS composite based on short glass fibers. Its matrix is a semi-crystalline high performance thermoplastic with high thermal stability, low water absorption (<0.02%) and high mechanical resistance and stiffness. For this study, the material was kindly supplied by Valeo Company in the form of injected plates.

This sampling method provides geometrically clean samples without negative edge effects. Experiments showed a very low dispersion of mechanical test results with this sampling method. It is important to note that, with this method there is no any effect of water on the properties of the composite for different reasons: the water absorption of PPS is very low and the time of this method is very short (<30 s). Besides, the temperature of aging is high (between 140 and 200°C) and at these temperatures all residual water will go out of the samples just at the beginning of aging tests.

The samples with a standard dog-bone dimension (see the reference 40) were put into ovens under different thermal aging temperatures (140, 160, 180, and 200°C, respectively). Total aging time was up to about 53:00 h. Samples were progressively taken out from ovens at different applied aging time for physicochemical and mechanical characterizations.

Characterization Methods

Microscopic Observations. A scanning electronic microscope (HITACHI 4800 SEM) has been used to investigate qualitatively the PPS composite microstructure and especially the fiber-matrix interface evolution.

Infrared Analysis. Fourier transform infrared (FTIR) spectrometry was used to characterize the extent of polymer oxidation, using a Nicolet impact 410 spectrophotometer in transmission mode. Measurements were made on spectra resulting from the accumulation of 32 runs, the resolution being 4 cm^{-1}. The absorbance of C=O group was converted to the concentration using a molar absorptivity of 300 L. mol^{-1}. cm^{-1} at the peak position (1,780 cm^{-1}) [41] and a molar absorptivity of 42 L.mol^{-1}. cm^{-1} at the peak position (2,923 cm^{-1}). Also the concentration of [C=O] or other degradation products can be calculated according to the Beer–Lambert law and the equation is as follows:

$$C = \frac{A}{e.\varepsilon} \qquad (1)$$

where, A is the absorbance for FTIR spectrum, e is the thickness of samples (20 μm) and ε is the molar attenuation coefficients (ε = 300 L. mol^{-1}. cm^{-1}).

Differential Scanning Calorimetry. The differential scanning calorimetry (DSC) measurements have been carried out with the DSC Q10 V9.0 Build 275TA Instruments (Guyancourt, France). The different samples were placed in hermetic aluminum capsules. The sample was heated up to 300°C with a temperature rate of 10°C/min in the atmosphere of Nitrogen (40 mL/min). To accumulate the degree of crystallinity of PPS/GF composite [42,43], the equation below was used:

$$X_C = \frac{\Delta Hf}{\Delta H_f^0 * \varphi} * 100\% \qquad (2)$$

where X_c is the crystallinity, ΔH_f is the sample enthalpy with unknown crystallinity and ΔH_f^0 is the pure reference PPS enthalpy (80 J/g), and φ is the percentage of PPS/GF in our material, with φ of 0.7 in this study.

Quasi-Static and Fatigue Test. Tensile properties and loading-unloading-reloading tests have been performed at room temperature using a MTS 830 hydraulic machine (capacity 10KN). The applied displacement rate was always 2 mm/min. Moreover, tension-tension fatigue tests also have been performed at different applied maximum stresses on the same machine. The minimum applied stress is always chosen to be equal to 10% of the maximum applied stress (R = 0.1) [44–47]. In this article, results of experiments performed at frequency of 10 Hz are presented. During cyclic loading, the plastic deformation and loss of stiffness evolution have been systematically evaluated. A previous paper [40] showed that under this frequency, the effect of

self-heating can be reasonably neglected in regard to the high values of transition temperatures for PPS.

RESULTS AND DISCUSSIONS

Thermal Aging Analysis

As mentioned earlier, the evolution of [C=O] concentration provides a very clear description of the oxidation process and the degree of degradation in the matrix. Figure 1a shows the FTIR results of C=O peaks after several exposition times at 200°C. One can note the location of the peaks at the wavenumber of 1,780, 1,735, and 1,710 cm^{-1}. Specifically, it can be classified into three different types of C=O group. One can note that there is an obvious increasing trend for the absorbance of C=O chemical group, which indicates that the PPS/GF composites are seriously oxidized at 200°C.

Another analysis shows that C-H peaks can be a second relevant indicator for thermal aging analysis of PPS composites. Figure 1b shows FTIR results of C-H peaks, corresponding to the wavenumber of 2,923 and 2,852 cm^{-1}, respectively. One can note
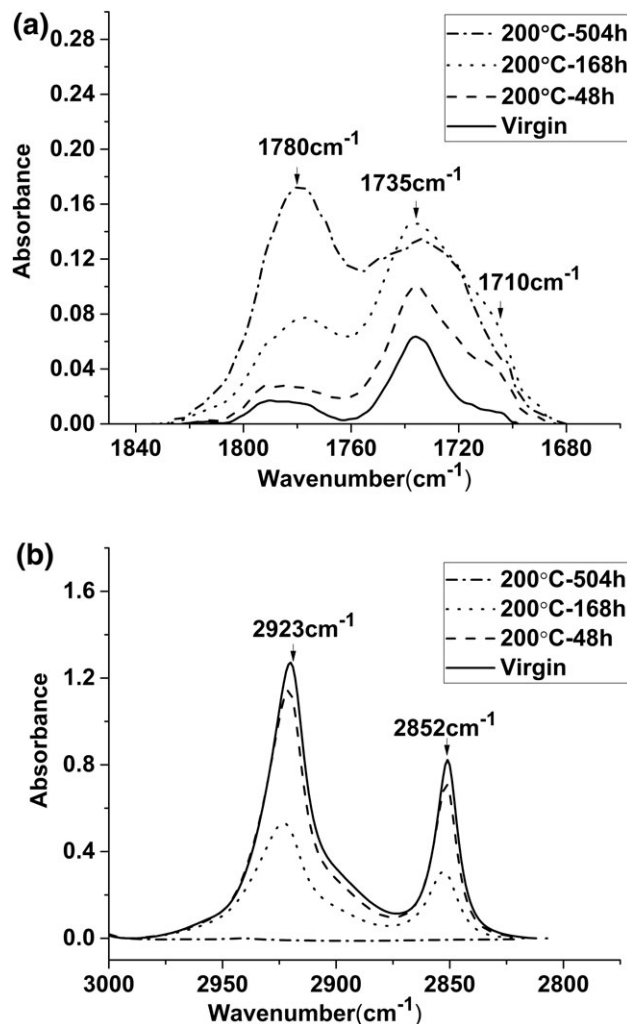
clearly that these peaks decrease sharply during oxidation due to the rupture of C-H chemical group. It can be also noticed that after an exposition of 504 h at 200°C, the C-H peaks tend to completely disappear. At this stage, the materials should be considered to be extremely degraded.

The [C=O] concentration evolution of PPS/GF composite under different oxidation temperatures at the peak positions of 1,780 cm^{-1} is shown in Fig. 2a. Classically, the oxidation process can be divided into three periods, induction, propagation, and termination. It can be seen that the induction time is very short (about 24 h) for the specimens aged at 200°C while this value significantly increases for the temperatures of 180 and 160°C (240 and above 1,100 h, respectively), and for 140°C, the induction time is very long (>2,000 h). Indeed, one can note that the induction time at temperatures of 180 and 160°C is about 10 and 45 times higher than the case in 200°C, respectively. Besides, the rate of propagation is very sharp for the oxidation temperature in 200 and 180°C. After less 1,000 h of oxidation in 200°C, the propagation tends to be saturated when the amount of oxidation products reaches a maximum. At 180°C, the saturation seems to
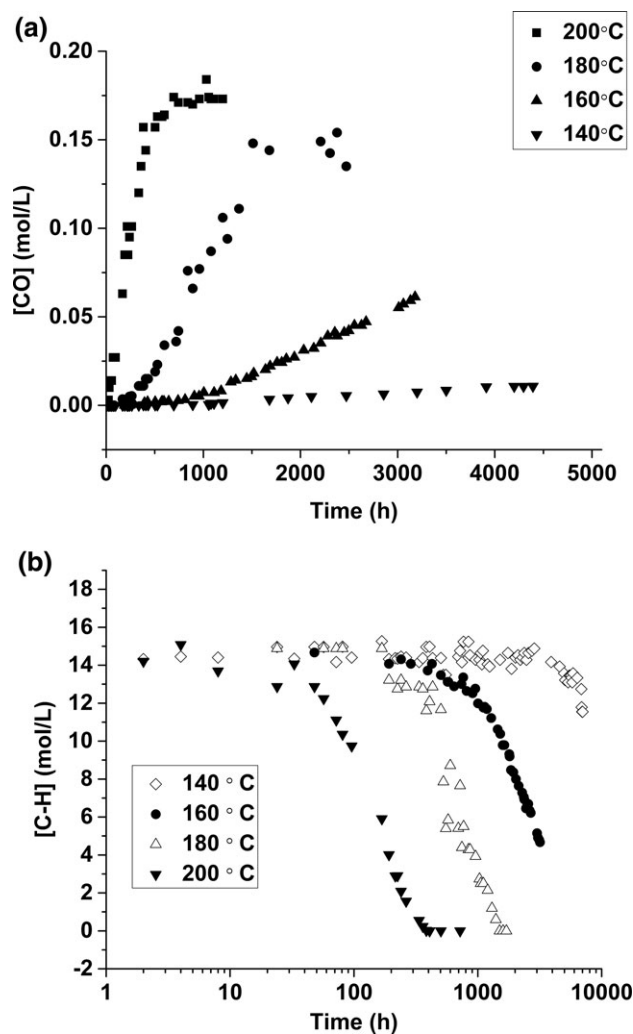

FIG. 1. (a) FTIR results of C=O peaks situated at 1,780, 1,735, and 1,710 cm^{-1}; specimens aged at 200°C. (b) FTIR results of C-H peaks situated at 2,923 and 2,852 cm^{-1}; specimens aged at 200°C.

FIG. 2. (a) Concentration evolution of [C=O] at 1,780 cm^{-1}, as a function of oxidation time under different oxidation temperatures (140, 160, 180, and 200°C). (b) Concentration evolution of [C-H] at the peak of 2,923 cm^{-1}, as a function of oxidation time under different oxidation temperatures (140, 160, 180, and 200°C).

be reached until 2,000 h of exposition. Comparatively, there is no comparable evolution and no stable plateau tendency observed for 140°C oxidation even after above 4,000 h of exposition. So, it can be concluded that, to the PPS/GF composite, the oxidation rate at 200 and 180°C are considerably harsher and faster than the cases of oxidation conditions of the temperature of 160 and 140°C. [C=O] concentration evolution analysis shows that induction time, oxidation kinetic, and saturation are obviously affected by temperature in the range from 140 to 200°C.

To complete the analysis, the evolution of [C-H] concentration obtained from the peak at 2,923 cm^{-1} is shown in Fig. 2b. According to this figure, one can note that at 200°C, the [C-H] concentration decreases sharply starting from 33 h. This analysis implies the induction time of [C-H] is slightly higher than that for [C=O] concentration. This delay indicates that these two mechanisms may occur simultaneous and are probably coupled. Moreover, one can note that after 360 h, the [C-H] bonds tend to completely disappear at 200°C. One can consider that, at this point, oxidation is over. Comparatively, the induction and termination points of oxidation at 180°C, are about 192 and 1500 h, respectively. This indicates that decreased oxidation temperature leads to significant delay of the induction and termination times. At 160°C, the induction time and termination time of C-H bond rupture tends to be longer than the case in 180 and 200°C. At 140°C, the corresponding oxidation phenomenon is too weak to detect until 5,000 h exposition according to the concentration of [C-H]. Until this time, [C-H] concentration still seems stable.

According to the analysis, one can note that the oxidation temperature can obviously affect the induction, propagation and termination time of the C-H bond rupture. Higher oxidation temperatures (e.g., 200°C) are more pronounced to the tendency of C-H bond rupture.

A complete discussion about the mechanism of thermal aging for PPS composite will be presented in future publication. However, the above information allows studying the effects of thermal aging on the mechanical behavior of PPS composite under four aging temperatures (140, 160, 180, and 200°C). Different aging times have been considered. One should be noticed in mind that the so called virgin sample corresponds to the virgin sample (23°C–0 h).

Evolution of Morphology

The effect of aging on morphology of polymer has been followed by measuring its degree of crystallinity during the time. Table 1 shows the evolution of the degree of crystallinity of the samples aged at 180 and 200°C. The result shows that the degree of crystallinity of polymer increases at the beginning of the aging period for 180 and 200°C. Then it decreases during second step before stabilizing during relatively long time.

This increase of degree of crystallinity has yet been observed during the aging of certain thermoplastic polymers [48,49]. This increase is due to the chain scission and the rearrangement of the morphology of the polymer. This increase in the degree of crystallinity will lead to the increase of strength and rigidity of the polymer.

Effects of Thermal Aging on Overall Mechanical Behavior

Hereafter, three types of tests have been considered:

- Tensile test [50,51]: The effects of aging on the stress–strain curves obtained by tensile tests are presented. The evolution of Young's modulus, failure stress and failure strain are plotted for different aging conditions: Tensile response is analyzed for an oxidation temperature of 200°C after various aging times of 0, 30, 50, 100, and 199 h.
- Loading-unloading test [52–54]: It is necessary to analyze the loss of stiffness and the plastic deformation evolution to understand the effect of aging conditions on the damage and deformation mechanisms. Loading-unloading tensile tests are performed at aging temperature of 200°C after various oxidation times of 0, 30, 50, 100, and 199 h.
- Fatigue loading [45,55–58]: Tension–tension fatigue tests have been performed at 10 Hz to compare the fatigue life time of PPS composite at various aging temperatures and times. Moreover, analysis of stiffness reduction and fractography during and after cyclic loading are presented. Fatigue behaviors on four kinds of oxidized samples at 140, 160, 180, and 200°C at different aging times have been analyzed. One can note that two loading amplitudes have been selected from the analysis of the Wöhler curve obtained on virgin sample [40].

Tensile Tests Analysis. Tensile tests results clarify the influence of aging on the mechanical properties of PPS composite (see Fig. 3a–c). It was shown an improvement of elastic modulus and failure stress during the first stage of exposition. Several authors have attributed this improvement to the crosslinking and crystallinity, depending on the temperature and the time of exposure [59,60]. To be clear, during aging process, molecular chain scission, post-crosslinking and increase of crystallinity can occur simultaneously in our PPS polymer material. Also, it should be noted that at the beginning of thermal oxidation, the post-crosslinking and increase of crystallinity are pronounced while extensively long time thermal oxidation mainly corresponds to chain scission and serious degradation of PPS polymer.

Table 2 gives more details about the relative values and standard deviation of tensile test results of PPS composite at different stage of aging at 200°C, which is obtained from the MTS machine.

As a result, after the first stage of exposition, a second stage of aging during which the effect of chain scission becomes predominant at the surface of the specimen, finally leading to loss of properties of the PPS composite especially in terms of loss of
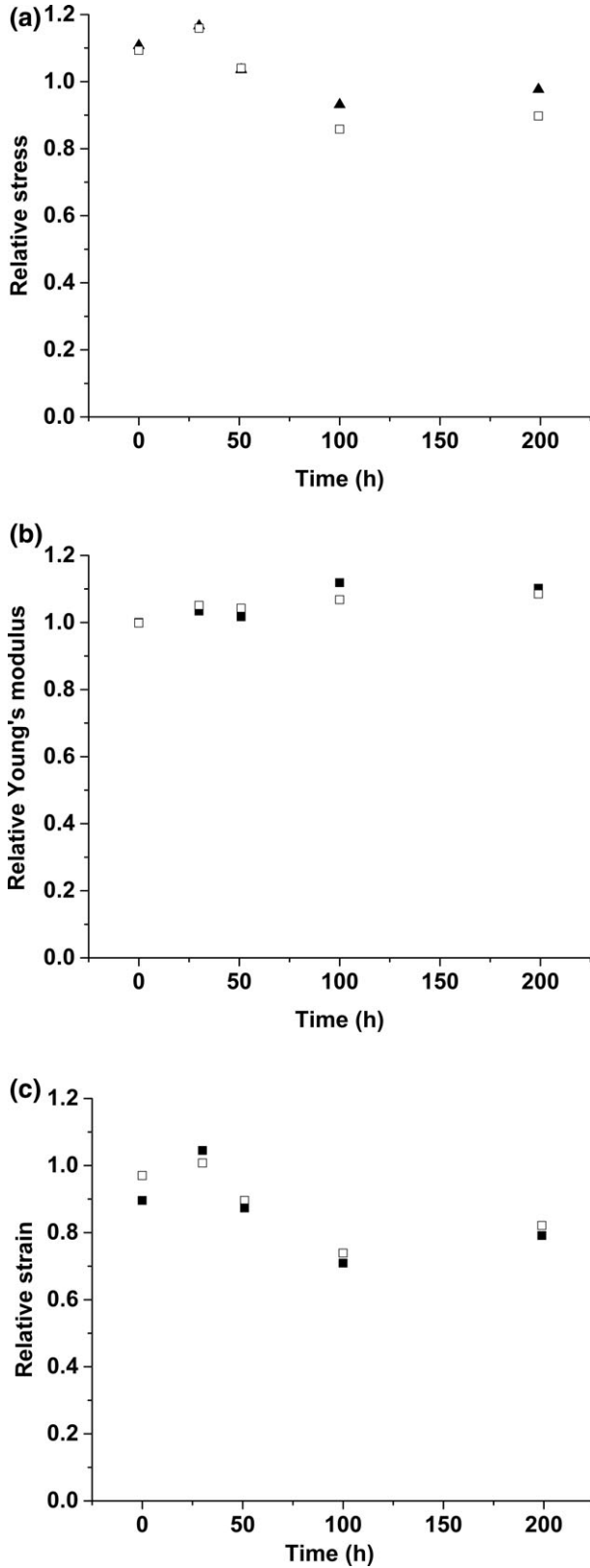
TABLE 1. The evolution of the degree of crystallinity of the samples aged at 180 and 200°C.

Time of aging (h)	Degree of crystallinity (%)	
	Aging temperature = 180°C	Aging temperature = 200°C
0	44.2	44.2
20	47.1	45.0
96	51.5	55.8
144	46.0	52.9
720	43.9	54.6
1,080	48.9	36.6

FIG. 3. (a) Evolution of relative failure stress during aging at 200°C: (Relative stress (resp. strain) = stress (resp. strain)/ultimate stress (resp. strain) obtained in virgin sample). (b) Evolution of relative Young's modulus during aging at 200°C: (Relative stress [resp. strain] = stress [resp. strain]/ultimate stress [resp. strain] obtained in virgin sample). (b) Evolution of relative failure strain during aging at 200°C: (Relative stress [resp. strain] = stress [resp. strain]/ultimate stress [resp. strain] obtained in virgin sample).

TABLE 2. Relative tensile results of PPS composites aged at 200°C.

Aging conditions	Time (h)	Relative failure stress σ/σ_0	Relative failure strain $\varepsilon/\varepsilon_0$	Relative Young's Modulus E/E_0
Virgin	0	1.13 ± 0.06	0.96 ± 0.07	1 ± 0.005
200°–30 h	30	1.17 ± 0.01	1.02 ± 0.02	1.01 ± 0.01
200°–51 h	51	1.04 ± 0.01	0.88 ± 0.01	1.05 ± 0.03
200°–100 h	100	0.92 ± 0.06	0.74 ± 0.05	1.09 ± 0.03
200°–199 h	199	0.94 ± 0.04	0.8 ± 0.01	1.1 ± 0.01

ductility. This issue can be explained by the fact that thermoplastics have linear or branched molecular structure and easily become more brittle because of chain scission or crosslinking and increase of crystallinity happening in aspect of chemical structure of PPS polymer.

From fracture surface analysis of virgin sample submitted to tensile loading until failure in Fig. 4a, it is obvious to indicate that fiber–matrix adhesion seems to be of very high quality, probably due to the presence of a coupling agent. Indeed, fibers have been pulled out in such a brittle way but still remain coated by a thin layer of PPS matrix.

Comparatively, in the case of aged sample at 200°C for 199 h, Fig. 4b, one can note that the residual matrix on the exposed surface of fibers and almost fibers surfaces are smooth. This indicates that the matrix degrades very seriously. Thermal aging has destroyed the matrix and leads to the separation of matrix and fibers, which in return reduces the mechanical retention of PPS original material.

Loading–Unloading Analysis. One can observe that, under monotonic loading, the predominant non-linear deformation mechanism seems to be the local plasticity of PPS matrix [40]. In order to quantify the possibility of plastic deformation and damage development, loading–unloading tensile test with progressive increase of the maximum stress have been performed in two cases: virgin samples and aged specimens at 200°C for 199 h (Fig. 5) shows the plastic deformation (ε_p) and loss of stiffness parameter (E/E_0) evolutions as a function of maximum stress for aged specimen. As it was shown above, the failure stress and strain decrease by aging. One can notice the relative stability of the Young's modulus which indicates no significant damage occurs during quasi-static loading (<1% decrease). Also, the plasticity increases about 5%.

Fatigue Behavior Analysis. *Effect of loading amplitude.* Figure 6 shows the Wöhler curves obtained in tension-tension fatigue tests at a frequency of 10 Hz for PPS-90° specimens at room temperature [40]. According to previous work, final failure and fatigue life of PPS/GF composite is highly dependent on the loading conditions (amplitude and frequency) and local microstructure. Bi-linear Wöhler curves emphasized the influence of the loading amplitude. More brittle failure was observed at high amplitude. For studying the effect of oxidation on fatigue behavior of the composite, iso-stress fatigue tests have been performed on the aged samples during the time. For these tests the choice of stress amplitude is very important. In order to have enough results during a reasonable time, for high aging temperatures, we must choose a low σ_r while for low aging temperatures; we must
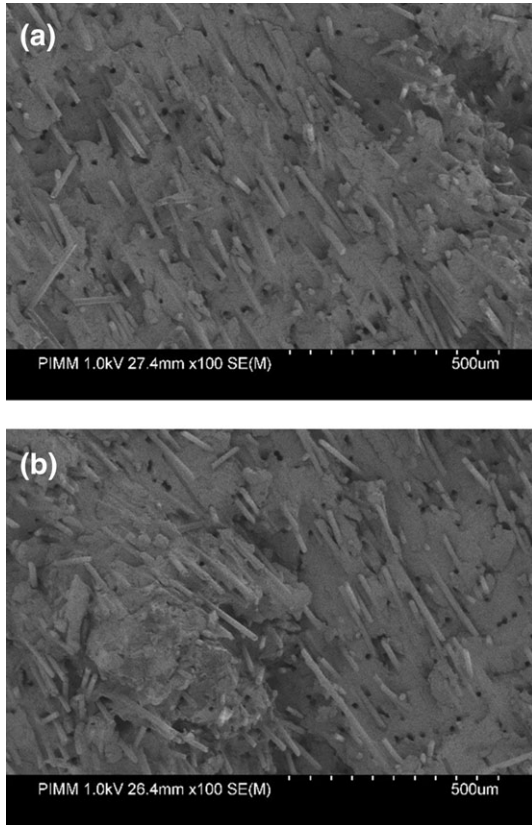
FIG. 4. (a) SEM micrograph of PPS/GF composite; fracture surface after tensile test of virgin sample. (b) SEM micrograph of PPS/GF composite; fracture surface after tensile test of aged sample at 200°C–199 h.
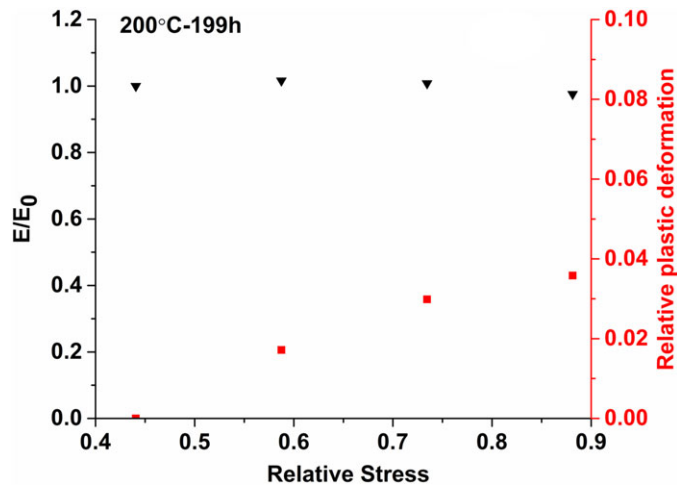

FIG. 5. The plastic deformation (ε_p) and loss of stiffness parameter (E/E_0) evolutions as a function of maximum stress: (Relative stress [resp. strain] = stress [resp. strain]/ultimate stress [resp. strain] obtained in virgin sample). [Color figure can be viewed at wileyonlinelibrary.com]
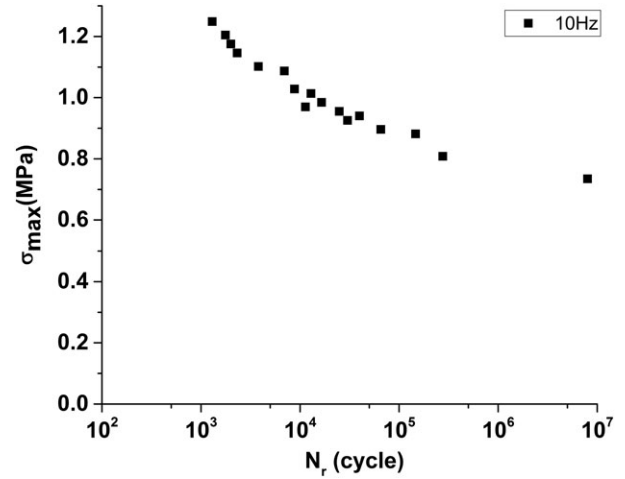

FIG. 6. Relative Wöhler curves of PPS/GF composite performed on PPS-90° specimens under tensile-tensile fatigue loading at the frequency of 10 Hz and room temperature, $R = 0.1$ (Relative stress = stress /ultimate stress obtained in virgin sample after tensile test [$\sigma_{ultimate-virgin}$]).

-virgin and $\sigma_{ultimate-virgin}$ (see Fig. 7). One can notice that the cycle number decreases with the loaded amplitudes increasing. In particular, the applied amplitude of 0.6 $\sigma_{ultimate-virgin}$ favors to a higher cycle (maximum to about 10^7 cycle) while one can also notice that the considerable reduction of cycle number with the amplitude of $\sigma_{ultimate-virgin}$, from 1.4×10^4 to 1.2×10^3 with an oxidation time of approximately 250 h. From Fig. 7, one can also note that the lifetime reduction rate is increased from the tests with loading amplitude from 0.6 $\sigma_{ultimate-virgin}$ to $\sigma_{ultimate-virgin}$. Results show the fatigue lifetime sharply decreases by aging time increasing in the case of loading amplitude of 0.6 $\sigma_{ultimate-virgin}$. Also the temperature of 180 °C favors an obvious diminution of fatigue cycle number with the increasing oxidation time.

Effect of Thermal Aging Temperature. Figure 8 shows the fatigue lifetime evolution as a function of oxidation time under different oxidation temperatures of 140, 180, and 200°C. One can note that fatigue lifetime reduction rate increases with thermal aging temperature. Indeed, at 200°C the fatigue lifetime is submitted to a very sharp decrease. This indicates the 200°C is very harsh to destroy the mechanical properties of PPS materials. This is to say, the fatigue lifetime is very sensitive to the oxidation temperature and decided by the thermal aging conditions.

Fatigue Behavior Coupled With Oxidation Phenomenon. Figure 9 shows the relation between N_r and [CO] in different oxidation temperatures. One can note that generally it can be divided into two zones, high oxidation temperatures (e.g., 200 and 180°C) and moderate temperatures (140 and 160°C). For the same rupture cycle number (N_r), one can see the moderate temperatures produce less [CO] amount while the high temperatures correspond to more [CO]. However, it needs to be noted that the large amount of [CO] in high temperatures is produced in a short time since the induction time for high oxidation temperature is very short and quick, which can be referred to the relative section above in this article.

Considering our PPS polymer material subjected to dynamic loading, the samples aged at high temperature will consume a short time to reach degradation while the low temperature will take more time to appear the same degree of degradation. Comparatively, the
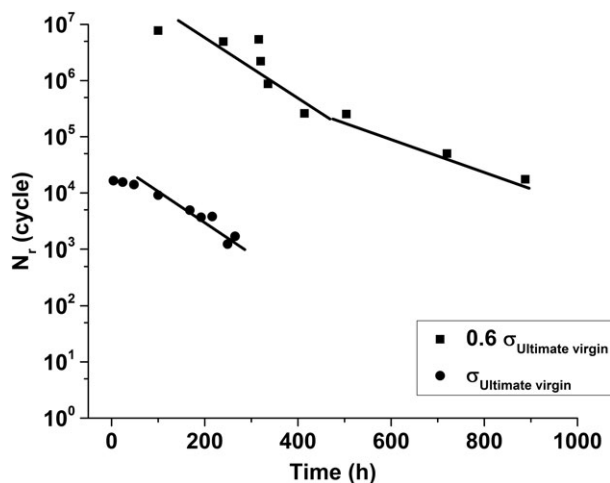
choose a high σ_r. So in the basis of the Wöhler curves for the study of fatigue behavior during aging at high temperatures (180 and 200°C) and also at low temperatures (140 and 160°C) for comparison, we have chosen $\sigma_r = 0.6$ $\sigma_{ultimate-virgin}$.

In order to study the fatigue lifetime of aged PPS composite at 180°C at different aging times tension-tension fatigue tests have been performed at different loading amplitudes of 0.6 $\sigma_{ultimate-}$

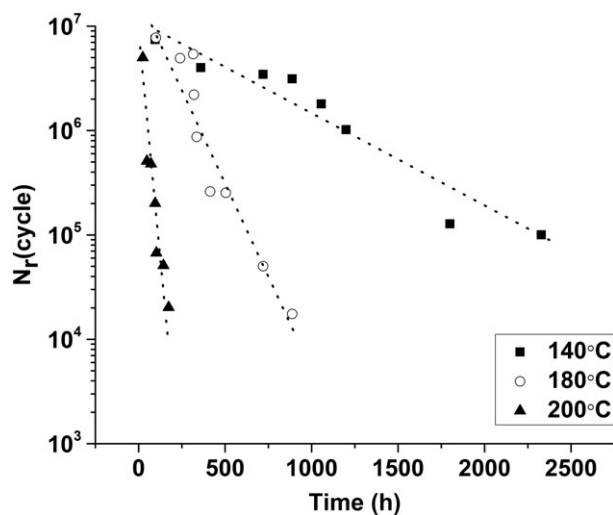FIG. 7. Effect of aging and loading amplitude on fatigue lifetime of samples aged at 180°C (f = 10 Hz).

FIG. 8. Effect of aging temperature on fatigue lifetime; fatigue tests at 10 Hz and loading amplitudes of 0.6 $\sigma_{ultimate-virgin}$.
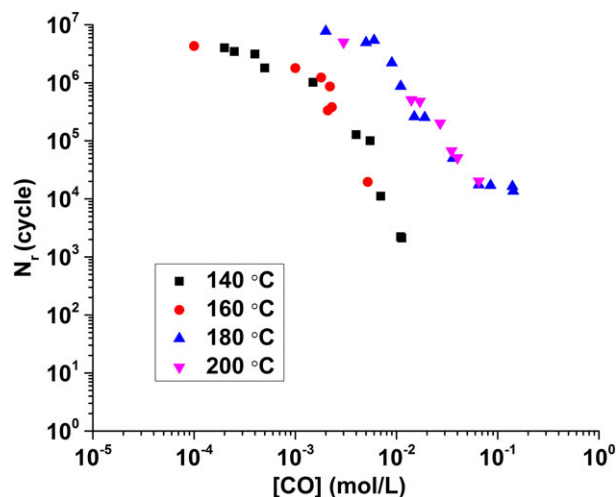

FIG. 9. Relation between N_r and [CO] in different oxidation temperatures. [Color figure can be viewed at wileyonlinelibrary.com]

[CO] can stand for the degradation degree. When the same cycle number was applied until rupture, the high temperature leads to more degradation, which is equivalent to high [CO] while the value for low temperature is small. Moreover, one can see that Nr decreases sharply with the increase of [CO], not only in the case of high temperatures (180 and 200°C), but also in the case of low temperatures (140 and 160°C).

CONCLUSION

PPS/GF composite was tested after oxidation at different temperatures (140, 160, 180, and 200°C) until approximately 5,300 h under tensile, loading–unloading and cyclic loading. The main results are as follows:

The oxidation rate increases by increasing the temperature. At 200°C it is considerably harsher and faster than at 140°C and this difference is related to the exothermic nature of global apparent activation energy of oxidation reactions.

Tensile behavior of sample aged at 200°C exhibited that at the beginning of oxidation from 0 to 30 h, the tensile behavior stays its mostly original retention. This is mainly due to the post-crosslinking and also to the increase of the degree of crystallinity of PPS. After then, the tensile strength decreases sharply almost of its 25% strength during 200 h. One can note that the relative Young's modulus slowly increases at the beginning of oxidation and this trend tends to be constant with the thermal oxidation time increasing. This also proves the crosslinking and increase of crystallinity exist during the oxidation process. Moreover, the strain has a consistent decrease. This indicates the material tends to be brittle during oxidation, showing a decreasing elongation.

Loading–unloading tests presented that the PPS/GF composite has an evident nonlinear elasticity-limited plasticity, not only for virgin sample, but also for aged samples.

Fatigue analysis of aged samples showed that the fatigue lifetime decreases with the loaded amplitudes increasing. The cycle number for aged samples has an obvious decreasing trending due to oxidation, and this trend tends to be more excessive with the oxidation temperature and oxidation time increasing. PPS/GF composite will lose its fatigue performance obviously at the beginning of oxidation and the fatigue performance will tend to be worse with the oxidation process going further.

REFERENCES

1. H.W. Hill and D. Brady, *Polym. Eng. Sci.*, **16**, 831 (1976).
2. L.C. López and G.L. Wilkes, *Polymer*, **30**, 882 (1989).
3. L. Caramaro, B. Chabert, J. Chauchard, and T. Vu-Khanh, *Polym. Eng. Sci.*, **31**, 1279 (1991).
4. M. Favaloro, "Properties and Processes of Linear Polyphenylene Sulfide (PPS) for Continuous Fiber Composites Aerospace Applications," *SAE Aerotech Conf.*, Seattle, WA, Paper Number 2009-01-3242 (2009).

5. N. Christopher, J. Cotter, G. Knight, and W. Wright, *J. Appl. Polym. Sci.*, **12**, 863 (1968).
6. G. Ehlers, K. Fisch, and W. Powell, *J. Polym. Sci., Part A: Polym. Chem.*, **7**, 2955 (1969).
7. L. Yu, S. Bahadur, and Q. Xue, *Wear*, **214**, 54 (1998).
8. L.A. Gyurova and K. Friedrich, *Tribo. Int.*, **44**, 603 (2011).
9. Q. Zhao and S. Bahadur, *Wear*, **217**, 62 (1998).
10. Z. Jiang, L.A. Gyurova, A.K. Schlarb, K. Friedrich, and Z. Zhang, *Compos. Sci. Technol.*, **68**, 734 (2008).
11. K. Stoeffler, S. Andjelic, N. Legros, J. Roberge, and S. B. Schougaard, *Compos. Sci. Technol.*, **84**, 65 (2013).
12. Y. Yang, H. Duan, S. Zhang, P. Niu, G. Zhang, S. Long, X. Wang, and J. Yang, *Compos. Sci. Technol.*, **75**, 28 (2013).
13. L. Lopez and G. Wilkes, *J. Macromol. Sci., Part C*, **29**, 83 (2012).
14. B.G. Risch, *Syst. Comput. Japan*, **35**, 1 (1994).
15. M.Ö. Bora, O. Çoban, T. Kutluk, S. Fİdan, and T. Sinmazçelİk, *Polym. Compos.*, **39**(5), 1604 (2016).
16. J. Edmonds Jr and H. Hill Jr, US Patent 3354129, 1967, in *Chem. Abstr*, pp. 13598 (1968).
17. R.T. Young and D.G. Baird, *Compos. B. Eng.*, **31**, 209 (2000).
18. X. Han, H. Ding, L. Wang, and C. Xiao, *J. Appl. Polym. Sci.*, **107**(4), 2475 (2008).
19. R. Black, C. List, and R. Wells, *J. Appl. Chem.*, **17**, 269 (1967).
20. J. Scobbo and C. Hwang, *Polym. Eng. Sci.*, **34**, 1744 (1994).
21. S.G. Pantelakis, C.V. Katsiropoulos, and P. Lefebure, *J. Appl. Polym. Sci.*, **107**, 3190 (2008).
22. L. Perng, *Polym. Degrad. Stab.*, **69**, 323 (2000).
23. J.Y. Cao and L.S. Chen, *Polym. Compos.*, **26**, 713 (2005).
24. J. Zhou, A. D'Amore, Y. Yang, T. He, B. Li, and L. Nicolais, *Appl. Compos. Mater.*, **1**, 183 (1994).
25. I. De Baere, W. Van Paepegem, and J. Degrieck, *Polym. Test.*, **32**, 1273 (2013).
26. I. De Baere, W. Van Paepegem and J. Degrieck, in *15th European Conference on Composite Materials (ECCM15-2012)*. Ghent University, Department of Materials Science and Engineering (2012).
27. I. De Baere, W. Van Paepegem, C. Hochard, and J. Degrieck, *Polym. Test.*, **30**, 663 (2011).
28. K. Tanaka, K. Oharada, D. Yamada, and K. Shimizu, *Int. J. Fatigue*, **92**, 415 (2016).
29. D. Backe and F. Balle, *Compos. Sci. Technol.*, **126**, 115 (2016).
30. J.F. Mandell, D. Huang, and F. McGarry, *Polym. Compos.*, **2**, 137 (1981).
31. R. Růžek, M. Kadlec, and L. Petrusová, *Int. J. Fatigue*, **113**, 253 (2018).
32. B. Vieille and W. Albouy, *Int. J. Fatigue*, **80**, 1 (2015).
33. W. Albouy, B. Vieille, and L. Taleb, *Int. J. Fatigue*, **63**, 85 (2014).
34. D. Kytýr, T. Fıla, J. Valach, and M. Šperl, *U.P.B. Sci. Bull.*, **75**, 157 (2013).
35. R. Sakin and I. Ay, *Mater. Des.*, **29**, 1170 (2008).
36. M. Alqam, R.M. Bennett, and A.-H. Zureick, *Compos. Struct.*, **58**, 497 (2002).
37. H. Rinne, The Weibull Distribution: A Handbook, Chapman and Hall/CRC, Boca Raton (2008).
38. R. Bedi and R. Chandra, *Compos. Sci. Technol.*, **69**, 1381 (2009).
39. T. Philippidis and A. Vassilopoulos, *Compos. Sci. Technol.*, **60**, 2819 (2000).
40. P. Zuo, R. Benevides, M. Laribi, J. Fitoussi, M. Shirinbayan, F. Bakir, and A. Tcharkhtchi, *Compos. B. Eng.*, **145**, 173 (2018).
41. G. Lisa, C. Hamciuc, E. Hamciuc, and N. Tudorachi, *J. Anal. Appl. Pyrolysis*, **118**, 144 (2016).
42. D. Brady, *J. Appl. Polym. Sci.*, **20**, 2541 (1976).
43. J.E. Spruiell, A review of the measurement and development of crystallinity and its relation to properties in neat poly (phenylene sulfide) and its fiber reinforced composites[R]. ORNL (2005).
44. M. Shirinbayan, J. Fitoussi, N. Abbasnezhad, F. Meraghni, B. Surowiec, and A. Tcharkhtchi, *Compos. B. Eng.*, **131**, 8 (2017).
45. V. Bellenger, A. Tcharkhtchi, and P. Castaing, *Int. J. Fatigue*, **28**, 1348 (2006).
46. E.A. Toubia and A. Elmushyakhi, *Mater. Des.*, **131**, 102 (2017).
47. W. Zhang, Z. Zhou, B. Zhang, and S. Zhao, *Mater. Des.*, **66**, 77 (2015).
48. L. Boukezzi, S. Rondot, O. Jbara, and A. Boubakeur, *Radiat. Phys. Chem.*, **149**, 110 (2018).
49. C. Han, E. Sahle-Demessie, A.Q. Zhao, T.I. Richardson, and J. Wang, *Carbon*, **129**, 137 (2018).
50. B. Yang, L. Lu, X. Liu, Y. Xie, J. Li, and Y. Tang, *Mater. Des.*, **131**, 470 (2017).
51. N. Abbasnezhad, A. Khavandi, J. Fitoussi, H. Arabi, M. Shirinbayan, and A. Tcharkhtchi, *Int. J. Fatigue*, **109**, 83 (2018).
52. S.M. Daghash and O.E. Ozbulut, *Mater. Des.*, **111**, 504 (2016).
53. A. Gosar and M. Nagode, *Int. J. Fatigue*, **43**, 160 (2012).
54. R.P. Skelton, *Int. J. Fatigue*, **26**, 253 (2004).
55. N.H. Mostafa, Z.N. Ismarrubie, S.M. Sapuan, and M.T.H. Sultan, *Mater. Des.*, **92**, 579 (2016).
56. M. Berer, D. Tscharnuter, and G. Pinter, *Int. J. Fatigue*, **80**, 397 (2015).
57. Y. Hu, H. Li, J. Tao, L. Pan, and J. Xu, *Polym. Compos.*, **39**, 1447 (2018).
58. L. Chen and B. Gu, *Polym. Compos.*, **39**(5), 1455 (2018).
59. S. Lee, D.-H. Kim, J.-H. Park, M. Park, H.-I. Joh and B.-C. Ku, *Advances in Chemical Engineering and Science*, **3**, 145 (2013).
60. R.T. Hawkins, *Macromolecules*, **9**, 189 (1976).